RSC Advances

ROYAL SOCIETY OF CHEMISTRY

www.rsc.org/advances

Journal Name RSCPublishing

COMMUNICATION

Facile fabrication of boron nitride nanosheets/amorphous carbon hybrid film for optoelectronic applications

Cite this: DOI: 10.1039/x0xx00000x

Received 00th January 2012,
Accepted 00th January 2012

DOI: 10.1039/x0xx00000x

www.rsc.org/

Shanhong Wan[a], Yuanlie Yu[b], Jibin Pu[a], Zhibin Lu[a]

A novel boron nitride nanosheets (BNNSs) /amorphous carbon (a-C) hybrid film have been deposited successfully on silicon substrates by the simultaneous electrochemical deposition, and showed a good integrity of this B-C-N composite film by the interfacial bonding. This synthesis can potentially provide the facile control of the B-C-N composite film for the potentially optoelectronic devices.

Two dimensional boron-carbon-nitrogen (B-C-N) ternary materials shows a series of electronic properties from insulation to semi-metallic in terms of nanosheet, nanoribbon and film, showing profound promise for optoelectronic devices, luminescent devices, transistors, and micro-electrical-mechanical system (MEMS), *etc.*.[1-3] Techniques for the synthesis of B-C-N ternary material are mostly chemical vapour deposition (CVD) and physical vapour deposition (PVD). As a consequence, a spectrum of polymorphic structures in such B-C-N system are often obtained associated with the homophilicity (C-C) or the heterophilicity (C-B, C-N and BN),[4] making the precise control of their chemical stoichiometry and geometry formidable is a challenging problem. Essentially, the band-gap of B-C-N system closely depends not only on the stoichiometry but also on the particular atomic arrangements,[5] it is thereby a challenging opportunity that if appropriate structure and best performance of well-mixed B-C-N system can be easily tuned by the complex variants during a facile film deposition.

Amorphous carbon (a-C), a wide-band gap, thin-film semiconductor, has been intensively studied for its application of the active layer in the photodetectors, electroluminescent devices and field emission displays.[6] In particular, by choosing different types and sizes of the doped component, one can obtain a nanocomposite carbon material with desired optoelectronic properties. Recent investigations on graphene/*h*-BN hetero-junctions of the structural similarity motivate the alloying of amorphous carbon and *h*-BN to achieve novel ternary B-C-N hybrid film,[7-9] e.g. nanoscale *h*-BN sheets doped into the a-C matrix of the promising optoelectronic layer.[10] However, the precise intermixing of BNNSs in a-C matrix and the interface integrity between them in such ternary material is far from understood.

Here, we report on the fabrication of B-C-N ternary films by a facile electrochemical deposition, which allows us to easily control the precise stoichiometry of this kind of B-C-N system and their electronic structure of the optoelectronic devices.

A schematic of two-step synthesis of B-C-N ternary films is shown in Fig.1. After ultrasonication, the obtained *h*-BNNSs in water (~0.1

mg/ml) show a milky white colour, especially this homogenous dispersion is stable and only a few of precipitation can be observed over a few days in Fig.1b. The corresponding characterizations of *h*-BNNSs can be found in the electronic supplement information. Two strong peaks at 1380 cm^{-1} and 810 cm^{-1} of Fourier transform infrared spectroscopy (FTIR) are the in-plane stretching of B-N rings and out-of-plane bending vibration of B-N-B rings of sp^2-hybridized, respectively, typical characteristics of *h*-BN.[11] Further, a peak of ~3414 cm^{-1} is attributed to the stretching signal of O-H, indicating a number of hydroxyl groups on the BNNSs surface.[12] The obtained *h*-BNNSs have an average grain size of around 100 nm, determined by transmission electron microscopy (TEM). The selected area electron diffraction (SAED) pattern corresponds to (100) plane and (002) plane of *h*-BN, respectively.[12] The electrolysis of the BNNSs/ methanol electrolyte is performed under the electric field of 2400 V/cm and at 60 ± 5°C. Finally a uniformly grey film with the thickness of about 1000 nm is obtained on the silicon substrate in Fig.1d.

In Fig.2, *h*-BNNSs are homogeneously dispersed in a-C matrix with a grain size of about 5 nm, and the adjacent nanocrystalline BNNSs is around 2 nm apart. Noted that there is no clear crystalline boundary among the mixing hetero-structure interfaces, in other word, carbon atoms probably interact with B or N atoms of BNNSs under the intensive electric field during the co-deposition process. The SAED pattern shows the asymmetric matrix spots with a d-spacing of 0.25nm, which well agrees with *h*-BN. And three distinct absorption peaks can be identified at ~188, ~284, and ~401 eV in the electron energy loss spectroscopy (EELS), which belongs to the *K*-shell ionization edges of B, C, and N, respectively.[13] Those values well support the sp^2-hybridized bonding among B, C and N atoms according to their sharp π*, forming novel B-C-N structure of this hybrid film. In this study BNNSs/a-C composite film is easily obtained by the simple electrolysis of *h*-BNNSs/methanol dispersion as expected. However, the grain size of *h*-BNNS in a-C matrix is greatly smaller than the obtained *h*-BNNS in water, it can be explained that the smaller the grain size of *h*-BNNS in methanol electrolyte, the easier the incorporation of *h*-BNNS into a-C matrix during the electrodepositing process.

Quantitative XPS analysis shows the atomic concentrations of B and N in a-C matrix is around 1.8 at %. In Fig.3b, the B1s spectrum can be well fitted with a dominant peak at 189.6 eV attributed to B=N bonding in *h*-BNNSs, and one peak positioned at 191.0 eV assigned to the B-O bonding state. [14] Because the electro-negativity of C atom is lower than that of N atom, the charge displacement from B to C is lower than that from B to N, the peak at ~188.8 eV is possibly from the bonding configurations of B and C.[15] From Fig.3a, the sp^2 B–N bonding in *h*-BN contributes to the peak at ~397.5 eV, and the other one at ~399.4 eV is in association with the C–N/C=N bonding.[14, 15] The B1s and N1s spectra both signify the graphitic B-N bonding of *h*-BNNSs. A further illustration of carbon bonding is shown by the fitted C1s spectrum in Fig.3c. A shoulder peak at ~283.8 eV is attributed to B-C bonds, which is consistent with BC_x compounds that shows the peak at 283.0 eV for B_4C.[16] The binding energy of ~284.5 eV can be assigned to C-C bonds, while the peak at ~285.4 eV is a combined contribution of C=C bonds and C=N bonds because of the highly electronegative nitrogen atoms.[17] For the peak at ~288.8 eV, it is believed to be related to sp^3 C–O bonding since some oxidation of surface often occurs. It indicates that the interfacial bonding along the heterostructural boundary of the hybrid film happens. Furthermore, an increasing value of the sp^2-C/sp^3-C ratio from 0.8 to 1.0 identifies more graphitic phase in hybrid film as compared to pure a-C film. As shown in Fig.3d and 3e, two fitted peaks at ~1361 and ~1580 cm^{-1}, an increasing intensity of D peak and a simultaneous G peak narrowing can be found as well as an increasing ratio of I_D/I_G from 0.38 to 2.96, which confirms the amorphous nature of film and,[10] more graphitic carbon domains appear in the hybrid film as compared with pure a-C film.

During the electrolysis, the methanol electrolyte is broken down by the high electric field between electrodes, generating CH_3^+ ions which will be absorbed on the negative electrode.[18] Thus there will be the bonding probability of methyl ions with B and N atoms in *h*-BN sheets during the simultaneous depositing process. A periodic DFT calculation using $DMol^3$ code is further conducted to calculate the adsorption energy of the CH_3^+ ions perpendicular to the *h*-BN structure: on the top of the boron and nitrogen atoms, respectively shown in Fig.4. After the optimization, the shorter distance between the adsorbed CH3+ radical and the plane of *h*-BN sheet are obtained, 1.734Å for CH_3^+-B (*h*-BN) and 1.559Å for CH_3^+-N (*h*-BN), respectively. The calculated results shows, the absorption energy of CH_3^+ group to the B atom (CH_3^+-B (*h*-BN)) is around -1442.36 kJ/mol, while the absorption energy of CH_3^+ group to the N atom (CH_3^+-N (*h*-BN)) is about -950.30 kJ/mol, indicating the chemisorption of CH_3^+. Concerning the polarity, a charge transfer from methyl (cationic) to *h*-BN sheet takes place by the

characteristic of the bending of the sheet in Fig.4, inducing an increment in the polarity of the sheets. Accordingly, in the case of the dipolar moment, the values of the CH_3^+-BN structure go from 4.3×10^{-3} to 8.3×10^{-3} Debye obtained from the N, while 4.3×10^{-3} to 9.5×10^{-3} Debye from the B, which is in agreement with the investigation reported.[19] These calculation results well supports CH_3^+can be chemically absorbed on *h*-BNNSs, probably forming B-C and C=N bonding.

As for the possibility of the co-deposition of *h*-BNNSs and a-C, it is undoubted that CH_3^+ ions are necessarily moved towards the silicon substrate of the cathode.[17] Meanwhile, *h*-BNNSs will be polarized under the effect of the intensive electric field of 2400 V/cm, and a charged density increases toward the longitudinal edges of *h*-BNNSs.[20] And it will be absorbed on the cathode surface, achieving the entrapment of *h*-BNNSs into the a-C matrix. As references say, *h*-BNNSs aligned themselves parallel to the electric field to minimize the electrostatic energy and to overcome the free energy of the system, which will play a template of the growth of graphitic carbon in a-C matrix.[21, 22] XPS and Raman analysis in this study well reveal more graphitic carbon presents in the hybrid film. Especially, during the co-deposition process the interfacial interactions of the cationic CH_3^+ of methanol chemically bonded onto *h*-BNNSs greatly contributes to the good integrity of BNNSs/a-C hybrid film.[23] Inherently the filler of *h*-BNNSs in the nanoscale often has a wrinkled sheet topology obtained from the exfoliation process, which will improve the mechanical interlocking of BNNSs with the 3D cross-linked a-C matrix.[23] In this study, the carbon atoms will bond with B, N atoms of *h*-BNNSs, forming C=N and/or B-C bonds along the BNNSs/a-C interface.[23] Noted that considerable amounts of –OH groups are chemically anchored onto B atoms of *h*-BNNNs during the exfoliation process in water medium,[24] thus making *h*-BNNSs surface more hydrophilic. Those above-mentioned aspects greatly ensure the co-deposition of *h*-BNNNs and CH^{3+} species from the stable dispersion, and finally forming a homogeneous distribution of h-BNNs in a-C matrix shown in Fig.2.

The integrity of the obtained B-C-N hybrid film can be identified by the improvement in the mechanical property of BNNSs/a-C hybrid films, using a nanoindentation test. The increase in hardness from 2.35 GPa to 5.76 GPa and Young's modulus from 44.35 GPa to 105.90 GPa is achieved by the incorporation of h-BNNSs into a-C matrix, this improvement in mechanical property closely depends on a good integrity of the nanocrystalline/amorphous hybrid film.[25, 26] This remarked heterostructure further allows us to readily modulate the electronic structure of BNNSs/a-C hybrid film and its optoelectronic property mainly by tuning the sheet or tube's concentration in the organic electrolyte. Moreover, some experiments have shown the band gap of B-C-N thin films depends on the relative C and BN fractions, however there has been a controversy concerning the structural properties of B-C-N thin films: some investigations indicates the partial segregation between C and BN,[27] while others propose the models in which C, B, and N atoms are mixed. [28] For instance, a considerable decrease of the band gap of BN nanomaterial can be tuned by the 10% C doping.[29, 30]

In conclusion, we synthesized a novel *h*-BNNSs/a-C hybrid film by the facile electrochemical deposition, which gives a new approach to facile fabrication of B-C-N ternary system. The interfacial bonding between carbon and *h*-BNNSs contributes to the high integrity of this hybrid film. This graphite-like *h*-BNNSs/a-C hybrid film shows the promising applications in optoelectronic devices.

Authors gratefully acknowledge the financial support of National Natural Science Foundation of China (No.51102247 and 51105352).

Notes and references

[a] State Key Laboratory of Solid Lubrication, Lanzhou Institute of Chemical Physics, Chinese Academy of Sciences, Lanzhou 730000, China. Fax: +86 931 4968163; Tel: +86 931 4968080; E-mail: shwan@licp.ac.cn. nano@licp.cas.cn. zblu@licp.cas.cn.

[b] Advanced Membrane and Porous Materials Center, Division of Chemical and Life Science and Engineering, King Abdullah University of Science and Technology, Thuwal 23955-6900, Saudi Arabia; E-mail: yuanlie.yu@kaust.edu.sa.

Electronic Supplementary Information (ESI) available: [details of any supplementary information available should be included here]. See DOI: 10.1039/c000000x/

1. J. W. Li and V. B. Shenoy, *Appl. Phys. Lett.*, 2011, **98**, 013105-1.
2. X. Wang, C. Zhi, L. Li, H. Zeng, C. Li, M. Mitome, D. Golberg and Y. Bando, *Adv. Mater.*, 2011, **23**, 4072.
3. M. Bernardi, M. Palummo, J. C. Grossman, *Phys. Rev. Lett.*, 2012, **108**, 226805-1.
4. X. Blase, H. Chacham, *B-C-N Nanotubes and Related Structures*: Yap, Y. K., Ed.; Springer: New York, 2009, pp. 83.
5. R. Arenal, X. Blase, A. Loiseaua, *Adv. Phys.*, 2010, **59**, 101.
6. C. Mathioudakis, M. Fyta, J. Phys.: Condens. Matter, 2012, 24, 205502-205509.

7. M. Bernardi, M. Palummo, J. C. Grossman, *Phys. Rev. Lett.*, 2012, **108**, 2268051.
8. P. Sutter, R. Cortes, J. Lahiri, E. Sutter, *Nano Lett*., 2012, **12**, 4869.
9. M. P. Levendorf, C. –J. Kim, L. Brown, et al, *Nature*, 2012, **488**, 627.
10. C. Mathioudakis, M. Fyta, *J. Phys.: Condens. Matter*, 2012, **24**, 205502.
11. R. B. Huang, Y. Y. Meng, Z. Zhu, S. J. Zhou, S. Y. Xie and L. S. Zheng, *J. Phys. Chem. C*, 2010, **114**, 13421.
12. Y. Lin, T. V. Williams, T. B. Xu, W. Cao, et al., *J. Phys. Chem. C*, 2011, **115**, 2679.
13. C. N. R. Rao, K. Raidongia, A. Nag, K. P. S. S. Hembram, U. V. Waghmare and R. Datta, *Chem.–Eur. J.*, 2010, **16**, 149.
14. B. Yao, S. Z. Bai, G. Z. Xing, K. Zhang and W. H. Su, *Phys. B*, 2007, **396**, 214.
15. Z. X. Cao, L. M. Liu and H. Oechsner, *J. Vac. Sci. Technol., B*, 2002, **20**, 2275.
16. M. K. Lei, Q. Li, Z. F. Zhou, I. Bello, C. S. Lee, S. T. Lee, *Thin Solid Films*, 2001, **389**, 194.
17. K. J. Boyd, D. Marton, S. S. Todrov, et al., *J. Vac. Sci. Technol. A*, 1995, **13**, 2110.
18. X.B. Yan, T. Xu, G. Chen, et al., *Carbon*, 2004, **42**, 3103.
19. N. Alem, R. Erni, C. Kisielowski, M. D. Rossell, W. Gannett, A. Zettl, *Phys. Rev. B*, 2009, **80**, 155425-1.
20. R. Pascoe, J. P. Foley, *Electrophoresis*, 2002, **23**, 1618.
21. C. A. Martin, J. K. W. Sandler, A. H. Windle, M. –K. Schwarz, W. Bauhofer, K. Schulte and M. S. P. Schaffer, *Polymer*, 2005, **46**, 877.
22. H.-B. Cho, M. Shoji, T. Fujiwara, T. Nakayama, H. Suematsu, T. Suzuki and K. Niihara, *J. Ceram. Soc. Jpn*, 2010, **118**, 66.
23. C. Y. Zhi, Y. Bando, C. C. Tang, et al., *Adv. Mater*. 2009, **21**, 2889.
24. Y. Lin, T. V. Williams, T. B. Xu, W. Cao, et al., *J. Phys. Chem. C*, 2011, **115**, 2679.
25. P. K. Chu, L. H. Li, *Mater. Chem. Phys*., 2006, **96**, 253.
26. Y. zhao, D. W. He, L. L. Daemen, T. D. Shen, et al., *J. Mater. Res*., 2002, **17**, 3139.
27. Y. Zhang, K. Suenaga, C. Colliex, S. Iijima, *Science*, 1998, **281**, 973.
28. D. Golberg, P. Dorozhkin, Y. Bando, M. Haregawa, Z. –C. Dong, *Chem. Phys. Lett*., 2002, **359**, 220.
29. S. Y. Kim, J. Park, H. C. Choi, et al., *J. Am. Chem. Soc.*, 2006, **128**, 6530.
30. O. Stephan, P. M. Ajayan, C. Colliex, et al., *Science*, 1994, **266**, 1683.

Figure captions

Fig.1 Schematic of two-step preparation of BNNSs/a-C hybrid film by sonication and electrolysis: commercially boron nitride powder (a), h-BNNSs in water after sonication (b), setup of electrolysis (c), and BNNSs/a-C hybrid film (d).

Fig.2 Microstructure of the *h*-BNNSs/a-C film: HRTEM image (a, b and c), the corresponding SAED pattern (c), and EELS spectrum of the film (d).

Fig.3 XPS analysis of *h*-BNNSs/a-C film, the curve-fitted N1s spectrum (a), B1s spectrum (b), C1s spectrum (c). The curve-fitted Raman spectra of a-C (d) and *h*-BNNSs/a-C (e) films.

Fig.4 The obtained configuration of CH_3^+ absorbed on *h*-BN sheet: perpendicular to the B atom (a), and perpendicular to the N atom (b).

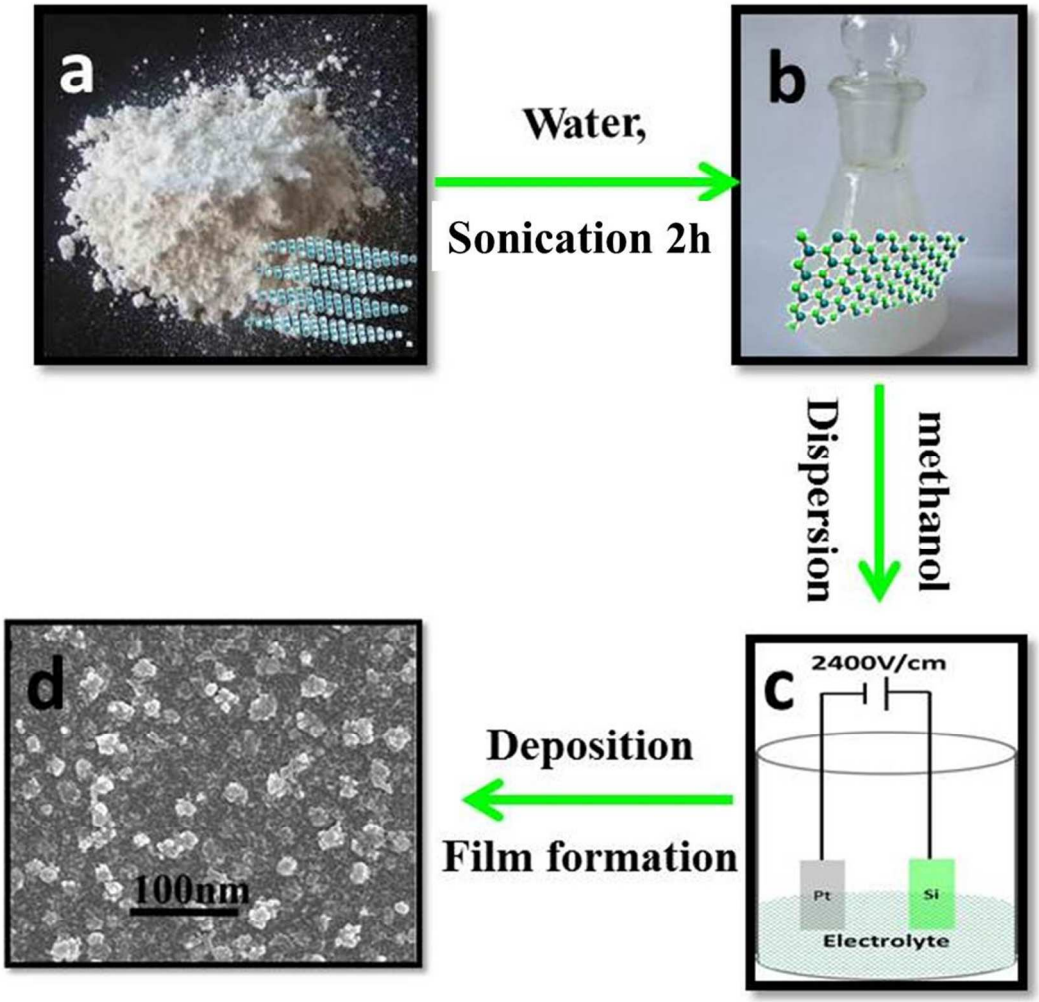

Fig.1 Schematic of two-step preparation of BNNSs/a-C hybrid film by sonication and electrolysis: commercially boron nitride powder (a), *h*-BNNSs in water after sonication (b), setup of electrolysis (c), and BNNSs/a-C hybrid film (d).

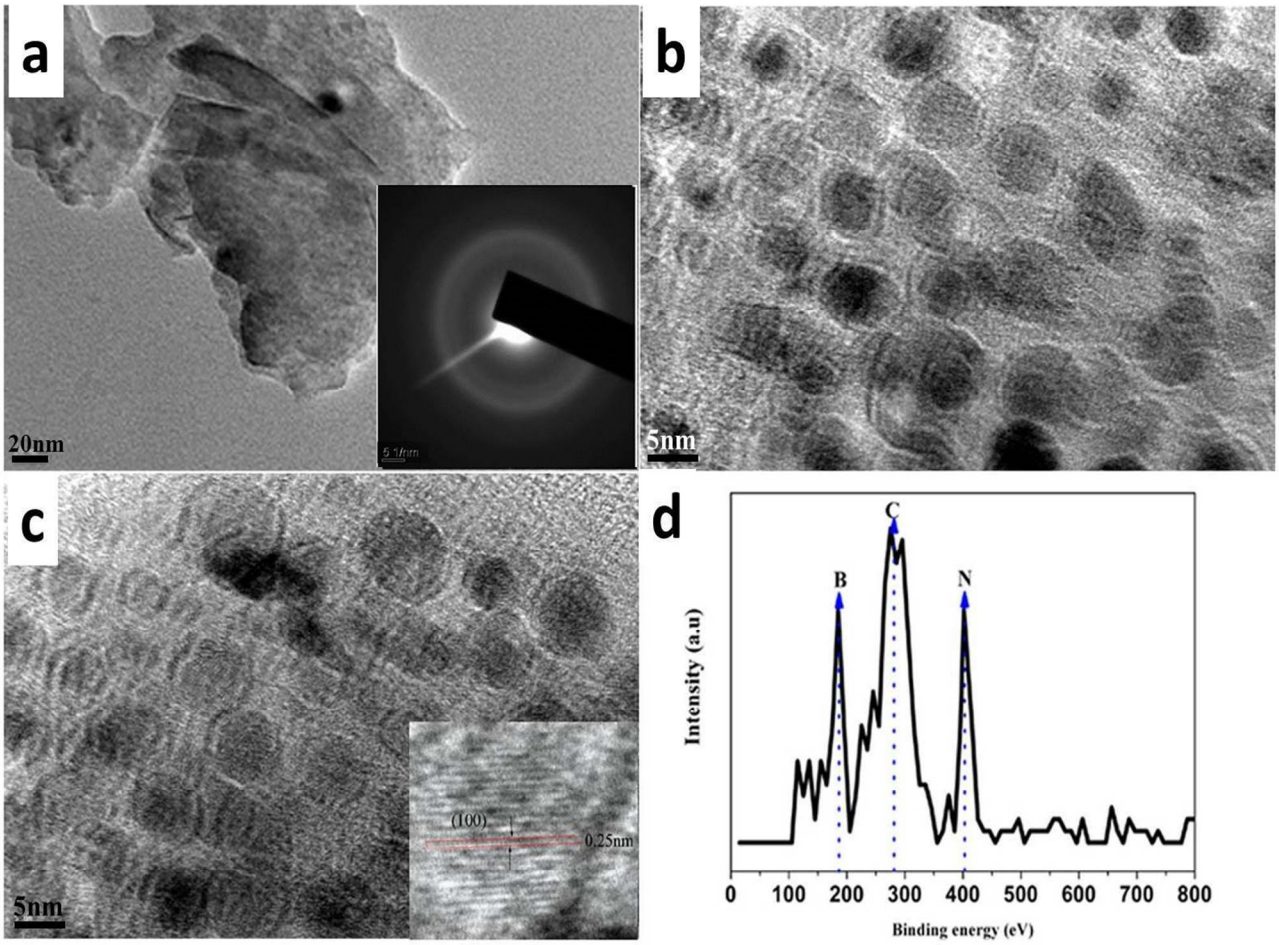

Fig.2 Microstructure of the *h*-BNNSs/a-C film: HRTEM image (a, b and c), the corresponding SAED pattern (c), and EELS spectrum of the film (d).

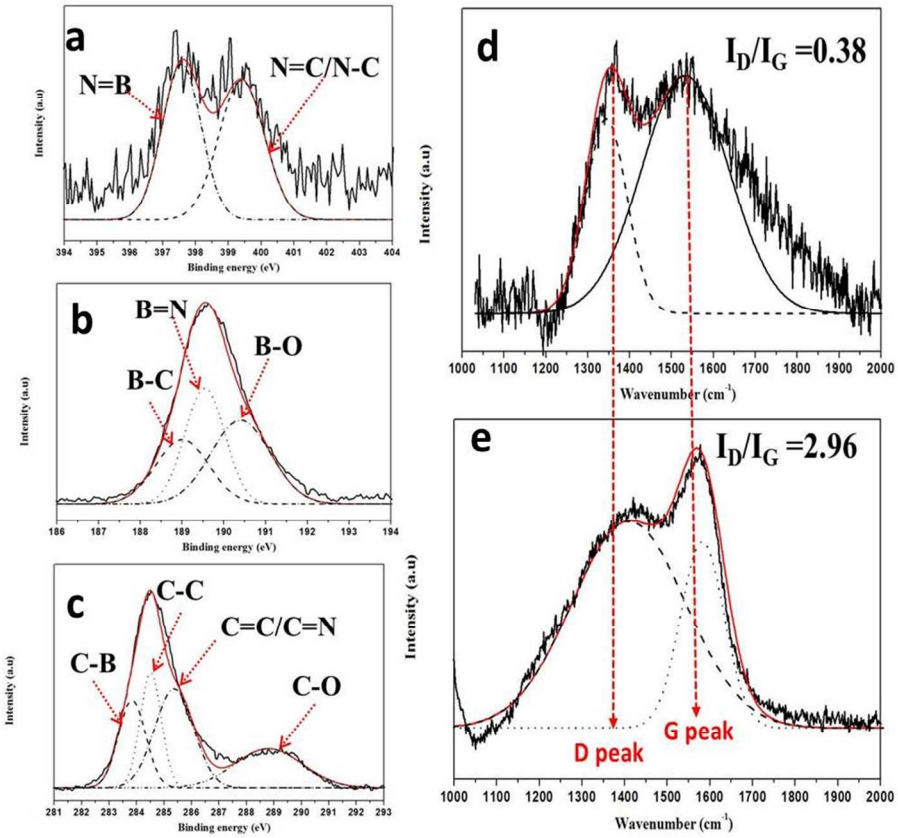

Fig.3 XPS analysis of *h*-BNNSs/a-C film, the curve-fitted N1s spectrum (a), B1s spectrum (b), C1s spectrum (c). The curve-fitted Raman spectra of a-C (d) and *h*-BNNSs/a-C (e) films.

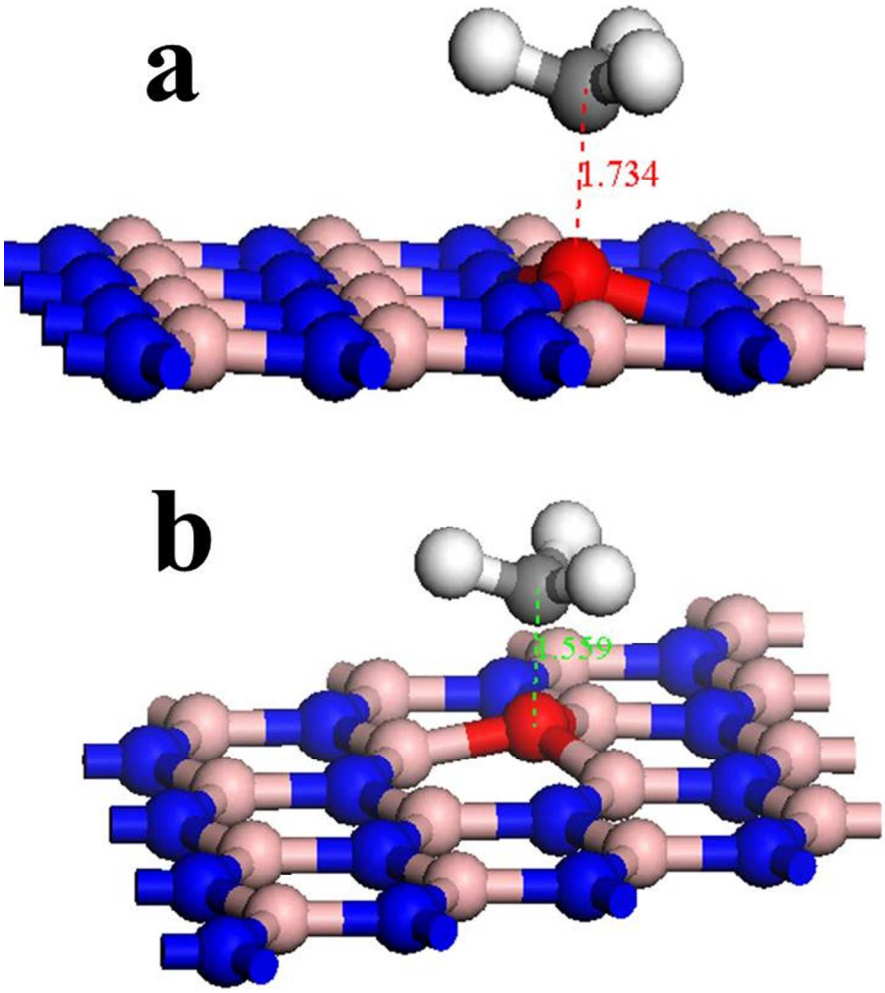

Fig.4 The obtained configuration of CH_3^+ absorbed on *h*-BN sheet: perpendicular to the B atom (a), and perpendicular to the N atom (b).